

A SURVEY OF ^{30}SiO EMISSION FROM EVOLVED STARS

SE-HYUNG CHO¹ AND NOBUHARU UKITA²

Received 1998 May 5; revised 1998 July 8

ABSTRACT

We present the first detection of $^{30}\text{SiO } v = 1, J = 1-0$ maser emission toward the Mira variable TX Cam among 18 surveyed evolved stars. The line width of this maser is much narrower than that of $^{30}\text{SiO } v = 0, J = 1-0$ masers and the intensity is also weaker, indicating that it is unsaturated. The detection of the ^{30}SiO maser emission in the lowest rotational transition of the first vibrationally excited state, together with nearly simultaneous observations of the large number of ^{29}SiO and ^{28}SiO masers, provides good constraints for establishing the SiO maser pumping model of TX Cam. The global features of ^{30}SiO and $^{29}\text{SiO } v = 1, J = 1-0$ lines are similar, but detailed characteristics, such as their half-widths, their peak intensity ratios of the $v = 1, J = 1-0$ line to the $v = 0, J = 1-0$ line, and their intensity variation with time, are different. New detection of the $^{30}\text{SiO } v = 0, J = 1-0$ and $J = 2-1$ lines is also reported in six evolved stars: TX Cam, R Cas, χ Cyg, W Hya, U Lyn, and WX Psc. They show a different masing characteristics of the ^{30}SiO that depends on both sources and transitions. This is probably related to a critical condition for masing.

Key words: circumstellar matter — masers — stars: late-type

1. INTRODUCTION

The rare Si isotope of SiO, ^{30}SiO , has been detected in evolved stars as a new circumstellar maser (Barcia, Alcolea, & Bujarrabal 1989). The relative abundances of the isotopic substitutions of SiO, in both the circumstellar and interstellar mediums, are comparable to the relative abundances of Si isotopes in the solar system, i.e., $^{29}\text{SiO}/^{30}\text{SiO} \sim 1.5$ and $^{28}\text{SiO}/^{30}\text{SiO} \sim 30$ (Penzias 1981; Kahane et al. 1988; Tsuji et al. 1994). Barcia et al. (1989) and Alcolea & Bujarrabal (1992) reported that the $^{30}\text{SiO } v = 0, J = 1-0$ maser appeared to be similar to ^{29}SiO masers in spectral structure and in the type of objects in which it is observed. Based on these similarities, Barcia et al. (1989) suggested that a similar pumping mechanism may work in both $^{30}\text{SiO } v = 0$ and $^{29}\text{SiO } v = 0$ masers. The ^{30}SiO rotational transitions in the vibrationally excited states, the $J = 4-3, v = 1$ and 2 lines, have been detected only toward VY CMa (Cernicharo & Bujarrabal 1992). The masing occurs very selectively in this rotational transition, somewhat similarly to that of ^{29}SiO masers (Cernicharo, Bujarrabal, & Lucas 1991). Other rotational transitions in the vibrationally excited states, especially the lowest rotational transition, have not been detected in any sources. In addition, observed sources and transitions in ^{30}SiO are quite limited. To investigate the detailed observational characteristics of ^{30}SiO masers, we have carried out simultaneous observations of ^{29}SiO and ^{30}SiO lines in evolved stars. In this paper, we report the first detection of the lowest rotational transition in the first vibrationally excited ^{30}SiO maser emission, including observational results of the $^{30}\text{SiO } v = 0, J = 1-0$ and $^{30}\text{SiO } v = 0, J = 2-1$ lines. The results of simultaneous observations of ^{29}SiO and ^{30}SiO will be presented in a forthcoming paper (Cho & Ukita 1998a).

2. OBSERVATIONS

The observations of the $v = 0, 1, J = 1-0$ and $v = 0, J = 2-1$ lines of ^{30}SiO and the $v = 2, 3, J = 1-0$ and $v = 1, J = 2-1$ lines of ^{29}SiO were made with the 45 m telescope of the Nobeyama Radio Observatory (NRO)³ in 1994 May and June. Two SIS receivers with a linearly polarized feed, S40 (32–50 GHz) and S100 (86–116 GHz), were used simultaneously. The single-sideband system temperature was 180–250 K for S40 and 250–500 K for S100 during our observations. Acousto-optical spectrometers with 37 kHz resolution (0.26 km s^{-1} at 43 GHz) and 40 MHz bandwidth were used. Aperture efficiencies were estimated to be 53% at 43 GHz and 39% at 86 GHz, respectively. The intensity calibration was made with the chopper wheel method. The intensity scale reported here is the antenna temperature T_A^* , corrected for atmospheric and ohmic losses (Ulich & Haas 1976). The antenna temperature is converted to flux density by using factors of 3.3 Jy K^{-1} at 43 GHz and 4.5 Jy K^{-1} at 86 GHz. Pointing was checked every hour by the sources themselves using a high electron mobility transfer receiver for 40 GHz band (HEMT40) receiver monitoring the $^{28}\text{SiO } v = 1, J = 1-0$ line. The pointing accuracy during our observations was within $5''$ in both azimuth and elevation. We selected 19 sources (12 M-type Mira variables, three S-type Mira variables, two supergiants, one OH/IR star, and Orion KL) that have shown relative strong $^{29}\text{SiO } v = 0, J = 1-0$ masers.

3. RESULTS AND DISCUSSION

$^{30}\text{SiO } v = 1, J = 1-0$ maser emission has been detected for the first time toward the Mira variable TX Cam among 18 surveyed late-type stars. Spectra are shown in Figure 1. The $^{30}\text{SiO } v = 0, J = 1-0$ and $^{30}\text{SiO } v = 0, J = 2-1$ lines have been also detected for the first time in TX Cam. Spectra and line parameters, simultaneously observed on

¹ Taeduk Radio Astronomy Observatory, Korea Astronomy Observatory, Whaam, Yusong, Daejeon 305-348, Korea; cho@hanul.issa.re.kr.

² Nobeyama Radio Observatory, National Astronomical Observatory, Minamimaki, Minamisaku, Nagano 384-13, Japan; ukita@nro.nao.ac.jp.

³ Nobeyama Radio Observatory is a branch of the National Astronomical Observatory, an interuniversity research institute operated by the Ministry of Education, Science, Sports, and Culture, Japan.

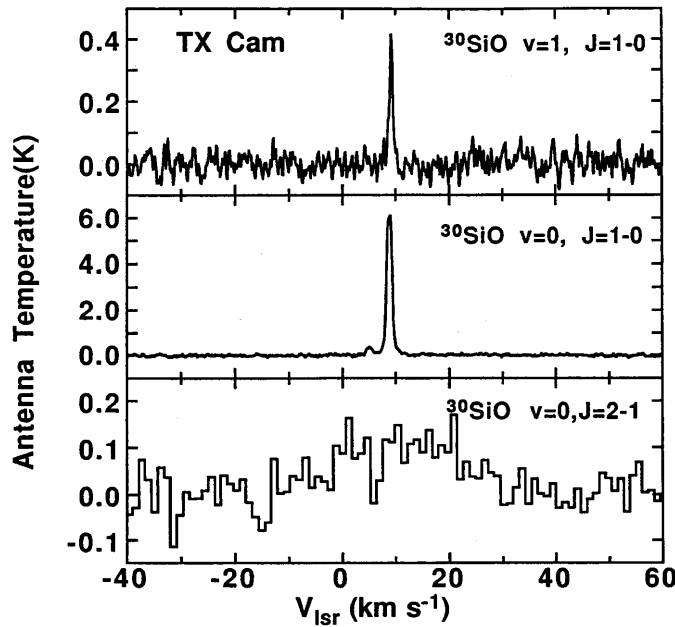


FIG. 1.—Simultaneously obtained spectra of ^{30}SiO from TX Cam on 1994 May 22 (optical phase 0.66). The spectral resolution is 37 kHz for the $^{30}\text{SiO } v=0, 1, J=1-0$ lines and 148 kHz for the $^{30}\text{SiO } v=0, J=2-1$ line. Antenna temperature of 1 K corresponds to a flux density of 3.3 and 4.5 Jy at 43 and 86 GHz, respectively.

1994 May 21 (phase 0.66), of ^{28}SiO and ^{29}SiO masers toward TX Cam are also presented in Figure 2 and Table 1. Observational results are summarized in Tables 1 and 2. We quote the date and optical phase relative to the visual maxima, transition, peak antenna temperature, rms, peak velocity, and integrated antenna temperature in the tables. New detections are indicated on the transition of observed sources. Optical phase was calculated from observed optical maximum data provided by the American Associations of Variable Star Observers (AAVSO) (J. A. Mattei 1994, private communication). The $^{30}\text{SiO } v=0, J=1-0, 2-1$ spectra and line parameters except those for TX Cam, are presented in Figures 3 and 4 and Table 2, respectively. We have also got new detections of ^{30}SiO emission in five evolved stars: R Cas, χ Cyg, W Hya, U Lyn, and WX Psc. For 10 other surveyed sources (W And, R Aqr, T Cam,

W Cnc, U Her, R Hya, R Leo, GX Mon, WX Ser, and OH 231.8+4), no emission has been detected within a 3 rms noise level of 0.03–0.14 K.

3.1. Pumping Mechanism of ^{30}SiO Masers

By simultaneous observations of the $^{30}\text{SiO } v=0, 1, J=1-0$ and $v=0, J=2-1$ and $^{29}\text{SiO } v=2, 3, J=1-0$ and $v=1, J=2-1$ transitions, we have detected $^{30}\text{SiO } v=1, J=1-0$ maser emission for the first time from TX Cam with the 15th intensity ratio of the $^{30}\text{SiO } v=0, J=1-0$ line. These observational results, together with nearly simultaneous observations of the large number of ^{29}SiO and ^{28}SiO masers (Table 1), provide good constraints for establishing the SiO maser pumping model of TX Cam. Recently, Gonzalez-Alfonso & Cernicharo (1997) have developed a nonlocal radiative transfer code to study the effects of line overlaps and successfully explained most of the ^{29}SiO , ^{30}SiO , and high- v ^{28}SiO maser lines detected so far. They indicate that the line overlap that causes the $^{30}\text{SiO } v=0, J=1-0$ inversion also tends to favor the $v=1, J=1-0$ maser. Namely, the $v=1, J=1-0$ maser is also produced by overlap between $^{30}\text{SiO } (1, 1) \rightarrow (0, 0)$ and $^{29}\text{SiO } (1, 3) \rightarrow (0, 4)$ for the turbulence velocity, $V_{\text{turb}} = 0.5 \text{ km s}^{-1}$, in their model. But some overlaps reduce the $v=1, J=1-0$ line intensity or destroy the inversion of the $v=1, J=1-0$ line. This anti-inverting effect of overlaps seems to explain the observed lack of this line. The $v=1, J=1-0$ line was detected only toward TX Cam among the 18 surveyed late-type stars. Concerning the detection of the rare maser (the $^{30}\text{SiO } v=1, J=1-0$ line including the $^{29}\text{SiO } v=1, J=1-0$ line from TX Cam), it is interesting how the unusual infrared and chemical characteristics of this oxygen-rich star are related to the rare masers, as mentioned by Cho & Ukita (1995).

3.2. Differences between ^{30}SiO and ^{29}SiO Lines

The global features of ^{30}SiO and ^{29}SiO lines are similar, but their detailed characteristics are different. The half-width of the $^{30}\text{SiO } v=1, J=1-0$ line is 0.7 km s^{-1} , while the half-width of the $^{29}\text{SiO } v=1, J=1-0$ line is 0.5 km s^{-1} . The half-width of the $^{30}\text{SiO } v=1, J=1-0$ line is broader than that of $^{29}\text{SiO } v=1, J=1-0$, in spite of the expectation that the $^{30}\text{SiO } v=1, J=1-0$ line is narrower than that of ^{29}SiO . In addition, the ratio of the $^{30}\text{SiO } v=1,$

TABLE 1

^{30}SiO , ^{29}SiO , AND ^{28}SiO RESULTS TOWARD TX CAMELOPARDALIS

| Date (Phase) | Transition | Peak Antenna Temperature (K) | rms (K) | Peak Velocity (km s^{-1}) | Integrated Antenna Temperature (K km s^{-1}) |
|-------------------------|---------------------------------|------------------------------|---------|--------------------------------------|---|
| 1994 May 22 (0.66)..... | $^{30}\text{SiO } v=1, J=1-0^a$ | 0.4 | 0.03 | 9.1 | 0.3 |
| | $^{30}\text{SiO } v=0, J=1-0^a$ | 6.1 | 0.03 | 9.0 | 9.0 |
| | $^{30}\text{SiO } v=0, J=2-1^a$ | 0.1 | 0.04 | 11.5 | 3.1 |
| 1994 Jun 29 (0.73)..... | $^{30}\text{SiO } v=1, J=1-0$ | 0.4 | 0.07 | 9.3 | 0.4 |
| | $^{30}\text{SiO } v=0, J=1-0$ | 5.2 | 0.07 | 9.1 | 7.6 |
| | $^{30}\text{SiO } v=0, J=2-1$ | 0.1 | 0.06 | 8.5 | 2.0 |
| 1994 May 21 (0.66)..... | $^{29}\text{SiO } v=1, J=1-0$ | 0.8 | 0.07 | 9.3 | 0.4 |
| | $^{29}\text{SiO } v=0, J=1-0$ | 19.6 | 0.07 | 8.8 | 33.6 |
| | $^{29}\text{SiO } v=0, J=2-1$ | 0.5 | 0.16 | 6.1 | 3.3 |
| | $^{28}\text{SiO } v=3, J=1-0$ | 0.2 | 0.06 | 9.8 | 0.1 |
| | $^{28}\text{SiO } v=2, J=1-0$ | 31.6 | 0.06 | 8.7 | 165.4 |
| | $^{28}\text{SiO } v=2, J=2-1$ | 6.3 | 0.16 | 9.0 | 8.2 |
| | $^{28}\text{SiO } v=1, J=2-1$ | 9.9 | 0.09 | 8.9 | 29.9 |

^a New detections. Antenna temperature of 1 K corresponds to a flux density of 3.3 and 4.5 Jy at 43 and 86 GHz, respectively.

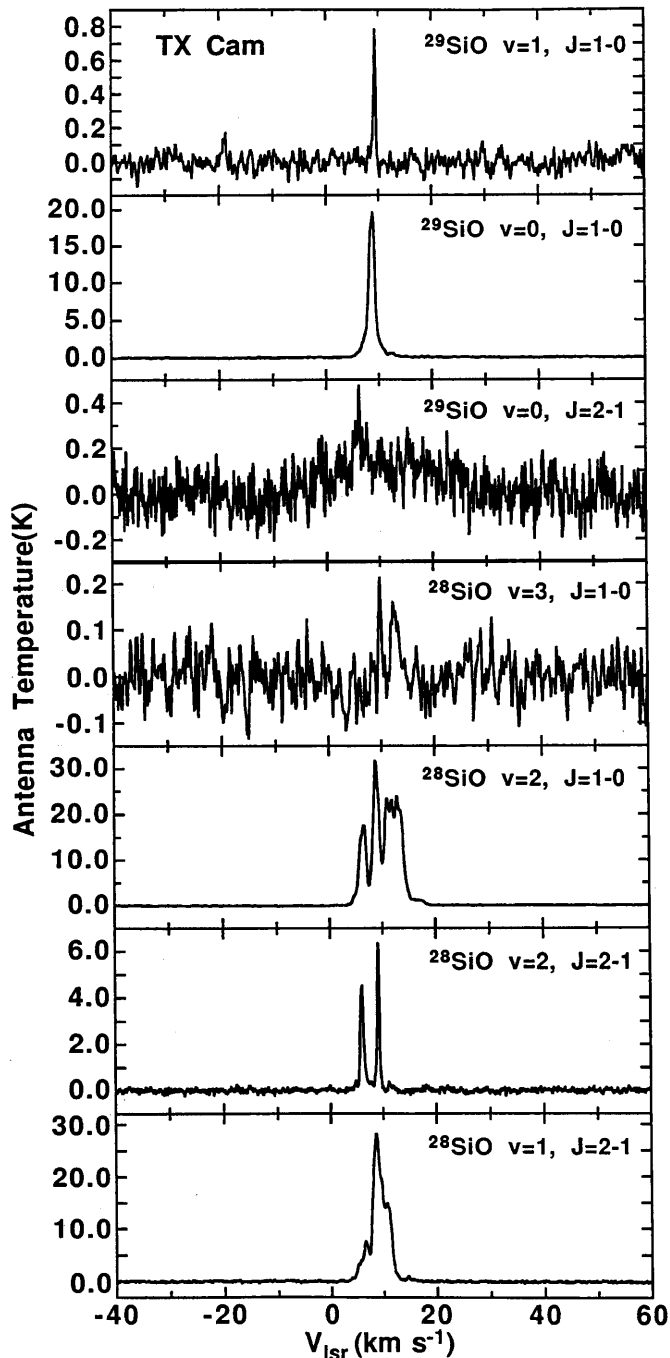


FIG. 2.—Simultaneously obtained spectra of ^{28}SiO and ^{29}SiO from TX Cam on 1994 May 21 (optical phase 0.66). Antenna temperature of 1 K corresponds to a flux density of 3.3 and 4.5 Jy at 43 and 86 GHz, respectively.

$J = 1-0$ line to the $^{30}\text{SiO } v = 0, J = 1-0$ (0.58) line is larger than that of the $^{29}\text{SiO } v = 1, J = 1-0$ line to $^{29}\text{SiO } v = 0, J = 1-0$ (0.38). These facts imply that the $^{30}\text{SiO } v = 1, J = 1-0$ line may be relatively more saturated than the $^{29}\text{SiO } v = 1, J = 1-0$ line, in spite of less abundance of ^{30}SiO . The peak velocity of the $^{30}\text{SiO } v = 1, J = 1-0$ line (9.1 km s^{-1}) is in good agreement with the peak velocity of $^{30}\text{SiO } v = 0, J = 1-0$ (9.0 km s^{-1}), while the peak velocity of $^{29}\text{SiO } v = 1, J = 1-0$ observed at the same phase is redshifted by 0.5 km s^{-1} from the peak velocity of $^{29}\text{SiO } v = 0, J = 1-0$ (Table 1). The peak antenna temperature of the $^{30}\text{SiO } v = 1, J = 1-0$ line ($T_A^* = 0.4 \text{ K}$) is about 1/15 of

that of $^{30}\text{SiO } v = 0, J = 1-0$ ($T_A^* = 6.1 \text{ K}$), while the peak antenna temperature of the $^{29}\text{SiO } v = 1, J = 1-0$ line ($T_A^* = 0.8 \text{ K}$) is about 1/25 that of $^{29}\text{SiO } v = 0, J = 1-0$ ($T_A^* = 19.6 \text{ K}$) at the optical phase of 0.66. We cannot find the peak intensity variation of the $^{30}\text{SiO } v = 1, J = 1-0$ maser between the optical phase of 0.66 and 0.73 (about one month later), differently from the weakening of the $^{30}\text{SiO } v = 0, J = 1-0$ maser. In the case of the $^{29}\text{SiO } v = 1, J = 1-0$ maser, we cannot detect the line within the 3 rms noise levels of 0.24 K at phase 0.73. By time-monitoring observations of TX Cam per month (from phase 0.56) (Cho & Ukita 1998b), the peak antenna temperature of the $^{29}\text{SiO } v = 1, J = 1-0$ line decreases by more than 30% every month. The observational characteristics between ^{29}SiO and ^{30}SiO maser lines are different in details, in particular, for the $v = 1, J = 1-0$ transition of both ^{29}SiO and ^{30}SiO . We expect that these observational characteristics will be explained by the different line overlap condition suggested by Gonzalez-Alfonso & Cernicharo's (1997) model. At phase 0.66, the peak intensity ratio of $^{29}\text{SiO } v = 0, J = 1-0$ to the $^{30}\text{SiO } v = 0, J = 1-0$ is 3.2 and the ratio of $^{29}\text{SiO } v = 1, J = 1-0$ to $^{30}\text{SiO } v = 1, J = 1-0$ is 2.0.

3.3. Velocity Structure of ^{30}SiO , ^{29}SiO , and ^{28}SiO

The $^{30}\text{SiO } v = 0, 1, J = 1-0$ masers appear within 0.3 km s^{-1} with respect to the stellar velocity, $V_{\text{LSR}} = 8.8 \text{ km s}^{-1}$. We adopted the peak velocity of the $^{29}\text{SiO } v = 0, J = 1-0$ maser emission as the stellar velocity based on Alcolea & Bujarrabal's (1992) observational results of this maser emission. These masers also show almost the same peak velocity after one month at phase 0.73. The $^{30}\text{SiO } v = 0, J = 2-1$ line shows a broad, thermal feature spreading from $V_{\text{LSR}} = -9 \text{ km s}^{-1}$ to 38 km s^{-1} , but a narrow spike at $V_{\text{LSR}} = 6.1 \text{ km s}^{-1}$ that appears in the $^{29}\text{SiO } v = 0, J = 2-1$ line (Fig. 2) does not appear in the ^{30}SiO line. We compare the velocity structure of the ^{30}SiO emission with those of ^{29}SiO and ^{28}SiO , which were nearly simultaneously obtained. As shown in Figure 2, we have detected the $^{28}\text{SiO } v = 3, J = 1-0$ line at phase 0.66, though this line was not detected at phase 0.56 (Cho & Ukita 1995). The $^{28}\text{SiO } v = 3, J = 1-0$ line shows the most redshifted component, compared with other maser lines in Table 1. The peak velocities of $^{30}\text{SiO } v = 0, 1, J = 1-0$ lines are slightly redshifted with respect to those of $^{29}\text{SiO } v = 0, J = 1-0$ and lie between $^{29}\text{SiO } v = 0$ and $^{29}\text{SiO } v = 1$. The peak velocities of the $^{28}\text{SiO } v = 2, J = 1-0$ and $v = 1, 2, J = 2-1$ lines, like those of the $^{30}\text{SiO } v = 0, 1, J = 1-0$ lines, are distributed within 0.3 km s^{-1} with respect to the stellar velocity, i.e., the peak velocity of $^{29}\text{SiO } v = 0, J = 1-0$ ($V_{\text{LSR}} = 8.8 \text{ km s}^{-1}$). Most of the above lines come at near the stellar velocity. However, peak velocities of $^{29}\text{SiO } v = 1, J = 1-0$ and $^{28}\text{SiO } v = 3, J = 1-0$ are redshifted, while the peak velocity of the $^{29}\text{SiO } v = 0, J = 2-1$ spike is blueshifted. It is difficult to discuss the systematic phenomenon based on the slight velocity difference obtained from only one object at two epochs. However, the location of the SiO line-emitting region close to the central star (Lane 1982; Diamond et al. 1994) and recent reports on SiO maser emission in relation to the stellar pulsation (Humphreys et al. 1996; Herpin et al. 1998) encourage in study of the SiO velocity structure connected with the stellar pulsation. Simultaneous, time-monitoring observations for multitransitions are required for understanding these kinds of problems connected with pulsation dynamics. In particular, multitransition observations,

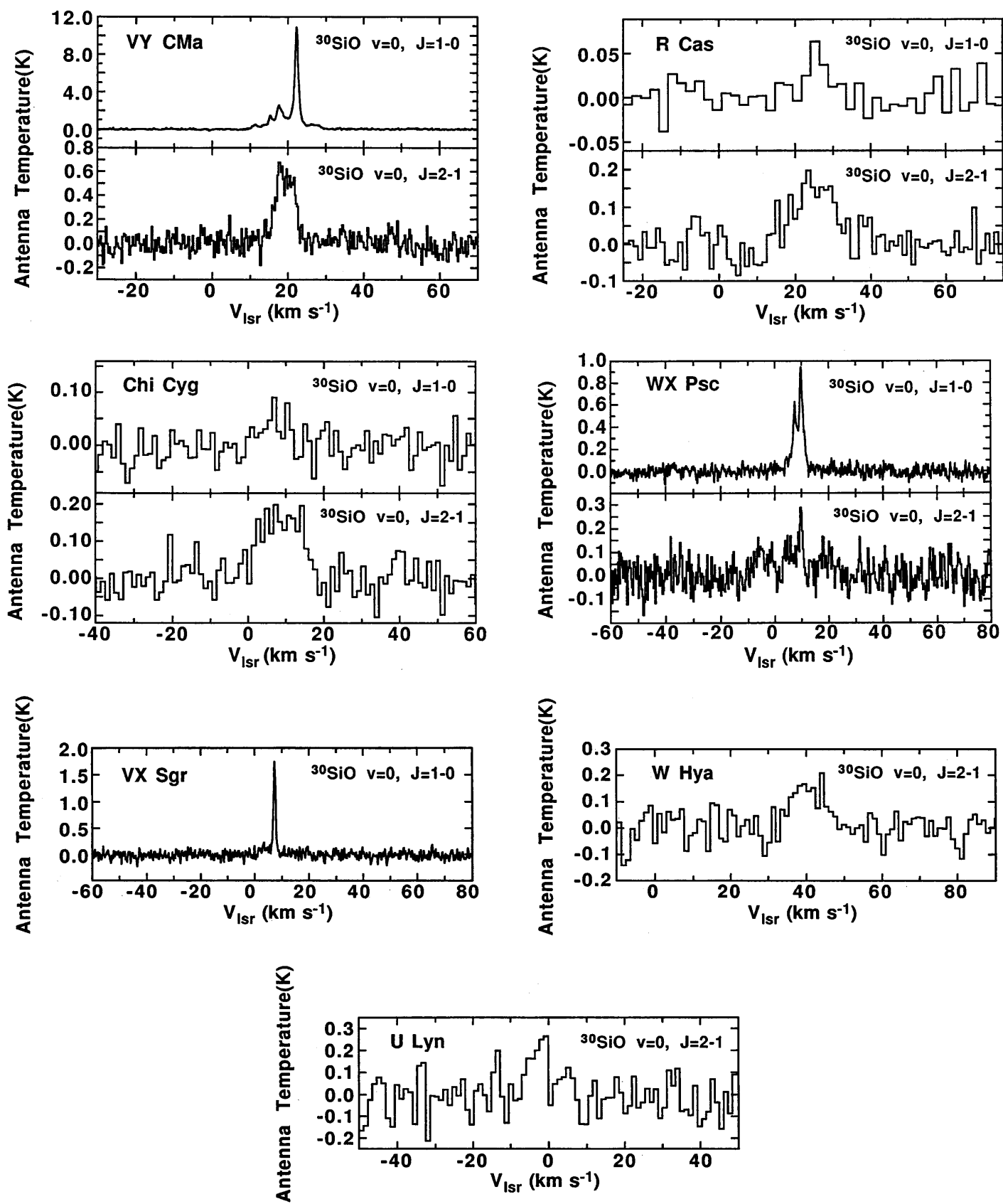


FIG. 3.—Simultaneously obtained spectra of $^{30}\text{SiO } v=0, J=1-0$ and $J=2-1$ transitions from evolved stars on 1994 May 22 and 24. The spectra are arranged in the same order as in Table 2. The spectral resolution is 222 kHz for the $^{30}\text{SiO } v=0, J=1-0$ line of R Cas, 37 kHz for spectra of WX Psc, and 148 kHz for others. Antenna temperature of 1 K corresponds to a flux density of 3.3 and 4.5 Jy at 43 and 86 GHz, respectively.

TABLE 2
³⁰SiO $v = 0, J = 1-0$ AND $J = 2-1$ RESULTS

| Source | Date (Phase) | Transition | Peak Antenna Temperature (K) | rms (K) | Peak Velocity (km s ⁻¹) | Integrated Antenna Temperature (K km s ⁻¹) |
|------------------|--------------------|--------------------------------------|------------------------------|---------|-------------------------------------|--|
| VY CMa | 1994 May 22 | ³⁰ SiO $v = 0, J = 1-0$ | 10.9 | 0.05 | 22.2 | 27.5 |
| | | ³⁰ SiO $v = 0, J = 2-1$ | 0.7 | 0.09 | 17.9 | 3.8 |
| R Cas | 1994 May 24 (0.64) | ³⁰ SiO $v = 0, J = 1-0^a$ | 0.1 | 0.02 | 25.3 | 0.3 |
| | | ³⁰ SiO $v = 0, J = 2-1^a$ | 0.2 | 0.04 | 24.9 | 2.3 |
| χ Cyg | 1994 May 24 (0.00) | ³⁰ SiO $v = 0, J = 1-0^a$ | 0.1 | 0.03 | 7.0 | 0.5 |
| | | ³⁰ SiO $v = 0, J = 2-1^a$ | 0.2 | 0.03 | 8.4 | 2.4 |
| WX Psc | 1994 May 24 | ³⁰ SiO $v = 0, J = 1-0^a$ | 0.9 | 0.06 | 9.8 | 3.1 |
| | | ³⁰ SiO $v = 0, J = 2-1^a$ | 0.4 | 0.13 | 9.9 | 2.0 |
| VX Sgr | 1994 May 24 (0.18) | ³⁰ SiO $v = 0, J = 1-0$ | 1.7 | 0.17 | 7.3 | 2.5 |
| W Hya | 1994 May 22 (0.94) | ³⁰ SiO $v = 0, J = 2-1^a$ | 0.2 | 0.06 | 40.5 | 1.6 |
| U Lyn | 1994 May 22 (0.17) | ³⁰ SiO $v = 0, J = 2-1^a$ | 0.2 | 0.09 | -2.6 | 1.4 |
| Orion KL | 1994 May 22 | ³⁰ SiO $v = 0, J = 1-0$ | 0.1 | 0.06 | 11.6 | 2.0 |
| | | ³⁰ SiO $v = 0, J = 2-1$ | 1.2 | 0.08 | 14.4 | 22.5 |

^a New detections. Antenna temperature of 1 K corresponds to a flux density of 3.3 and 4.5 Jy at 43 and 86 GHz, respectively.

TABLE 3
LINE PROFILE CHARACTERISTICS OF ³⁰SiO TRANSITIONS

| Source | ³⁰ SiO $v = 0, J = 1-0$ | ³⁰ SiO $v = 0, J = 2-1$ | ³⁰ SiO $v = 1, J = 1-0$ |
|------------------|------------------------------------|------------------------------------|------------------------------------|
| TX Cam | M | T | M |
| VY CMa | M | M | Not detected |
| R Cas | T | T | Not detected |
| χ Cyg | T | T | Not detected |
| WX Psc | M | T + M | Not detected |
| VX Sgr | M | Not detected | Not detected |
| W Hya | Not detected | T | Not detected |
| U Lyn | Not detected | T | Not detected |
| Orion KL | T | T + M | Not detected |

NOTE.—M indicates masing; T indicates thermal.

including those of high vibrationally excited states, will be helpful for tracing high energy regions close to the stellar photosphere, which is very sensitive to pulsation.

3.4. Line Profile Characteristics of ³⁰SiO Emission

We present the ³⁰SiO $v = 0, J = 1-0$ and $J = 2-1$ spectra of the detected sources in Figures 3 and 4. They show different characteristics of the line profiles depending upon both transitions and sources. This is probably because of the different masing condition of ³⁰SiO transitions acts. We show the line profile characteristics of the masing for sources in Table 3. There are five types of sources that exhibit different masing characteristics of ³⁰SiO. The sources W Hya and U Lyn show only the ³⁰SiO $v = 0, J = 2-1$ line with thermal characteristics at the time of our observations. Barcia et al. (1989) have detected the ³⁰SiO $v = 0, J = 1-0$ maser toward W Hya, but we did not detect it at phase 0.94. The ³⁰SiO $v = 0, J = 1-0$ transitions show maser emission in VY CMa, TX Cam, WX Psc, and VX Sgr, while this transition shows thermal-like emission in R Cas, χ Cyg, and Orion KL (Figs. 3 and 4). The ³⁰SiO $v = 0, J = 2-1$ lines of WX Psc and Orion KL show pedestal (or thermal) components with maser spikes, while this transition shows maser emission in VY CMa and shows thermal emission in TX Cam, R Cas, χ Cyg, W Hya, and U Lyn at our observation phase. We were not able to detect the ³⁰SiO $v = 0, J = 2-1$ emission toward VX Sgr, although we

detect the ³⁰SiO $v = 0, J = 1-0$ maser emission. From the above results (Table 3), we expect to determine the critical masing condition through the different masing characteristics of ³⁰SiO transitions according to sources. In addition, TX Cam seems to have a particular masing condition for ²⁹SiO and ³⁰SiO, compared with the other evolved stars, since both the rare ²⁹SiO $v = 1, J = 1-0$ and ³⁰SiO $v = 1, J = 1-0$ masers are detected only toward this star.

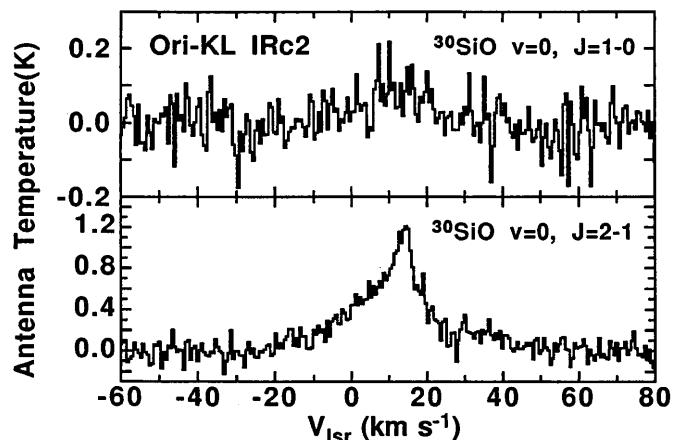


FIG. 4.—Simultaneously obtained spectra of ³⁰SiO from Orion KL on 1994 May 22. The spectral resolution is 74 kHz. Antenna temperature of 1 K corresponds to a flux density of 3.3 and 4.5 Jy at 43 and 86 GHz, respectively.

The observations were done while S.-H. C. was on sabbatical year at Nobeyama Radio Observatory. He would like to thank the Foreign Research Fellow (Visiting Professor) offered by the Ministry of Education, Science, Sports and Culture of Japan. This work was partially sup-

ported by Basic Research Grant 95-5100-005 and Star Project Grant 97-2-400-02 of the Korea Astronomy Observatory. In this research we have used information from the AAVSO International Database maintained at AAVSO Headquarters, 25 Birch Street, Cambridge, MA 02138.

REFERENCES

- Alcolea, J., & Bujarrabal, V. 1992, *A&A*, 253, 475
 Barcia, A., Alcolea, J., & Bujarrabal, V. 1989, *A&A*, 215, L9
 Cernicharo, J., & Bujarrabal, V. 1992, *ApJ*, 401, L109
 Cernicharo, J., Bujarrabal, V., & Lucas, R. 1991, *A&A*, 249, L27
 Cho, S.-H., & Ukita, N. 1995, *PASJ*, 47, L27
 ———. 1998a, in preparation
 ———. 1998b, in preparation
 Diamond, P. J., Kemball, A. J., Junor, W., Zensus, A., Benson, J., & Dhawan, V. 1994, *ApJ*, 430, L61
 Gonzalez-Alfonso, E., & Cernicharo, J. 1997, *A&A*, 322, 938
 Herpin, F., Baudry, A., Alcolea, J., & Cernicharo, J. 1998, *A&A*, 334, 1037
 Humphreys, E. M. L., Gray, M. D., Yates, J. A., Field, D., Bowen, G., & Diamond, P. J. 1996, *MNRAS*, 282, 1359
 Kahane, C., Gomez-Gonzalez, J., Cernicharo, J., & Guelin, M. 1988, *A&A*, 190, 167
 Lane, A. P. 1982, Ph.D. thesis, Univ. Massachusetts
 Penzias, A. A. 1981, *ApJ*, 249, 513
 Tsuji, T., Ohnaka, K., Hinkle, K. H., & Ridgway, S. T. 1994, *A&A*, 289, 469
 Ulich, B. L., & Haas, R. W. 1976, *ApJS*, 30, 247